
Enamel Structure on Children with Down Syndrome — An FT-IR Spectroscopic Study

V. Dritsa, D. Sgouros, K. Pissaridi, P. Bochlogyros,
M. Kyriakidou and V. Mamareli

Additional information is available at the end of the chapter

<http://dx.doi.org/10.5772/58909>

1. Introduction

Dental enamel and dentin comprise natural hydroxyapatite (HAP), including inorganic and organic compounds, define the quality and tolerance of these tissues. Enamel is the hardest tissue and differs significantly from dentin in organic and inorganic composition and structural organization. Enamel is composed of long and narrow crystals of carbonated hydroxyapatite, which are packed into parallel arrays. The organization of hydroxyapatite crystals during enamel formation regulates on the extracellular matrix proteins such as amelogenin, proteinases, ameloblastins and amelotin [1, 2]. Despite the low abundance of these proteins, they play essential roles in controlling the nucleation, growth, and organization of hydroxyapatite crystals. Specifically, amelogenin is phosphorylated enamel, specific glycoprotein, which may function as nucleation sites and substantially promote the apatite crystal growth [3]. Dentin is mainly composed of hydroxyapatite, an organic matrix rich in type I collagen and fluid which is similar to plasma. Due to its high organic and lower crystallinity, dentin is more porous and acid soluble tissue [4].

The development of dental diseases is attributed to the interaction of enamel with the oral environment, saliva and microorganisms. Enamel due to its highly mineralized structure is prone to microbial attack and can be dissolved and solubilized by acidic agents. Microbial adhesion to tooth surfaces, specifically enamel salivary pellicle is a general prerequisite for initiation of plaque formation. Microbial multiplication is the dominant feature in the build-up of dental plaque [5]. Plaque is a biofilm of densely packed bacteria, which regulates the exchange of nutrients and products of metabolism and demineralization between saliva and tooth surface. The pattern of bacterial colonization is dependent on the surface structure and topographic features of the tooth [6, 7]. Among the factors that affect plaque mineralization

and calculus formation, calcium plays an important role. Calcium is involved in the stabilization of the lipopolysaccharide (LPS) that constitutes the major component of the surface of gram-negative bacteria [8].

Due to the early stage of tooth formation, tooth morphology is related to genetic factors. Individuals with hereditary disorders such as Down syndrome (DS) have remarkably small teeth. The antero-posterior shortened palate, microdontia of permanent dentition, while some primary teeth are larger, altered crown morphology and shape, taurodontism and hypodontia spacing, agenesis, hypoplasia and hypocalcification are some common dental characteristics associated with DS [9-11]. Many studies have described that hypoplasia of enamel results in a reduced amount of enamel matrix and a decreased opacity of enamel layer, in patients with Down syndrome [9].

FT-IR spectroscopy has proven to be a fundamental and valuable technique in biology and medicine due to its high sensitivity to detecting changes in the functional groups belonging to tissue components such as lipids, proteins and nucleic acids [12]. It has been successfully applied in the study of various human tissues such as mineralized tissue, breast cancer, colon cancer, arteries, cartilage [13-17].

In this work, we analyze the structural and chemical characteristics of enamel as well as the appearance of bacteria in extracted teeth from children with dental abnormalities. Fourier transform infrared (FT-IR) spectroscopy and Scanning Electron Microscopy (SEM) were used for the determination of the structural changes in teeth. Teeth of children with no adverse medical history were used as a control group. Supragingival calculus was taken from both groups and was analyzed by spectroscopic analysis in order to investigate the influence of disease on the presence of bacteria.

2. Materials and methods

2.1. Teeth preparation

Ten teeth extracted from children (6-14 years) with Down syndrome were used in this study. Five teeth of children with no adverse medical history and five teeth from adults were used as a control group (Scheme 1).



Scheme 1. The extracted teeth were divided in four sections.

All extractions were done for orthodontic or periodontal reasons. After extraction, the teeth were rinsed with distilled water to remove blood remnants. Each tooth was carefully split into two with a low speed diamond saw. The enamel was separated using a hand-guided dental saw. The milled teeth powdered for used for FT-IR analysis.

2.2. FT-IR spectra

The FT-IR spectra were obtained with a Nicolet 6700 Thermoscientific spectrometer, connected to an attenuated total reflection, ATR, accessory. For each region a series of spectra were recorded and every spectrum consisted of 120 co-added spectra at a resolution of 4 cm^{-1} and the OMNIC 7.1 software was used for data analysis. All the spectra for each patient and region were obtained in the same way.

2.3. Scanning Electron Microcopy — SEM

Analysis of teeth morphology was performed by Scanning Electron Microcopy–SEM using a Fei Co at an accelerating potential 25 kV. Qualitative elemental data analysis of the samples was determined by EDX (Energy-dispersive X-ray spectroscopy).

3. Results and discussion

3.1. FT-IR spectroscopy

Figure 1 shows the comparison of the representative FT-IR spectra of enamel in healthy and DS patients. The spectra provide distinct features for the determination of the chemical composition and structure of the teeth.

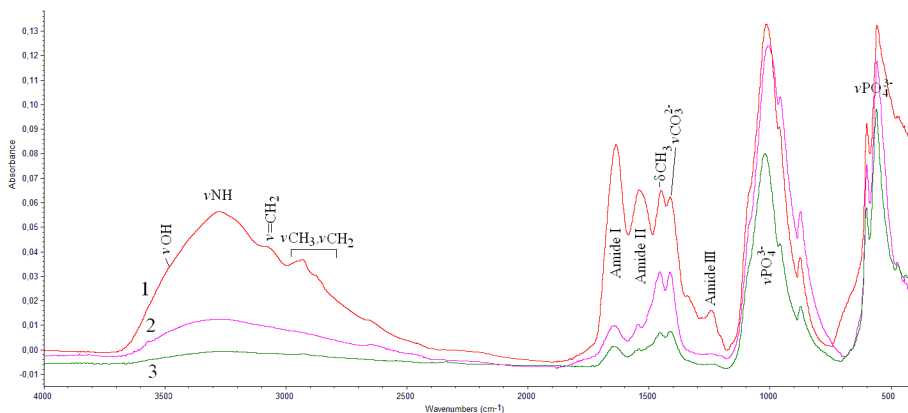


Figure 1. FT-IR absorption spectra of enamel obtained from healthy (1), DS (2) and adult (3) in the region $4000\text{--}400\text{ cm}^{-1}$.

In the region 4000-2500 cm^{-1} , enamel of DS patient showed a broad band at 3397 cm^{-1} , which is attributed to stretching vibration of hydroxyl group (νOH) of hydroxyapatite and crystalline water. In normal enamel, the absorption band at 3301 cm^{-1} shows a red shift compared to that of DS spectra, concerning that this band is assigned to hydroxyl group νOH -of hydroxyapatite. A second band was also determined at 3290 cm^{-1} due to the adsorption of the stretching vibration νNH group of Amide I. The band at 3070 cm^{-1} is assigned to the olefinic or aromatic stretching vibration of νCH group of aminoacids of collagenous proteins [18-20]. In the region 3000-2800 cm^{-1} , the bands of antisymmetric and symmetric stretching vibrations of methyl (νCH_3) and methylene (νCH_2) groups of enamelin and teeth proteins were indicated^{12,20}. In normal enamel the absorption band at 3301 cm^{-1} shows a red shift compared to that of DS spectra, concerning that this band is assigned to hydroxyl group νOH -of hydroxyapatite. A less intense band was observed in adult enamel improving the lower concentration of organic phase in accordance with literature data [13, 16, 21].

In the region 1800-400 cm^{-1} of the infrared spectra of enamel the observed absorption bands at 1651 cm^{-1} are dominated to Amide I group of proteins. In DS patients' spectra enamel indicated an intense band, which reveals that the mineralization of enamel has not been properly formed, recognized as an "imperfect osteogenesis" due to collagen defects [9]. Despite the fact that the level of collagen proteins is not rich, a low band was also indicated in the case of the control group, resulting that collagen is one of the basic components of enamel [1, 4]. The amide II absorption band was shown at 1544 cm^{-1} and had the highest absorbance in DS enamel. It is the second band of the peptide bond, and it arises mainly from the NH in-plane bending and the $-\text{CN}$ stretching vibration¹²⁻²¹. The Amide II band in enamel confirms that its organic substrate consists of collagen proteins. The analysis of the spectra by Fourier self-deconvolution was used to enhance resolution in the region 1800-1500 cm^{-1} (Fig.2).

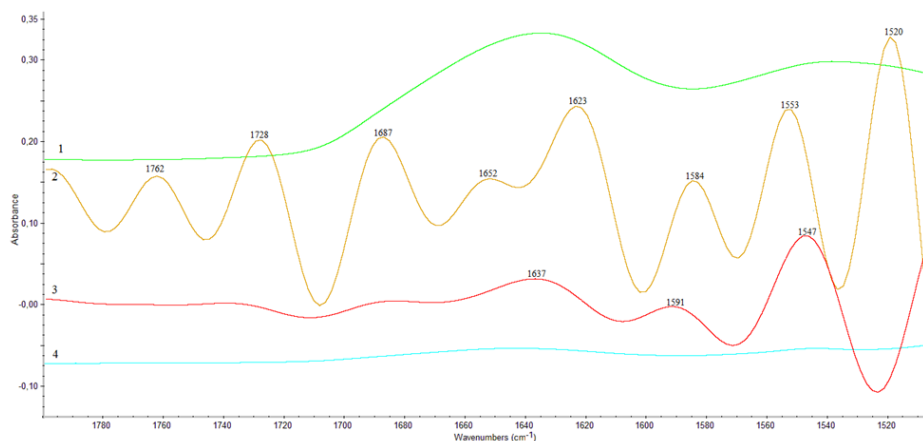


Figure 2. FT-IR spectra and deconvolution analysis in the region 1800-1500 cm^{-1})DS enamel2) Deconvolution analysis of DS enamel 3) Deconvolution analysis of healthy enamel 4) Healthy enamel.

Deconvolution of DS enamel revealed a number of absorptions in the amide bands. The band at 1762 cm^{-1} is attributed to stretching vibration of carboxyl groups (-COO^-). The shift of this band is related to the Ca^{2+} binding to COO^- groups [1].

The band at 1728 cm^{-1} is due to the stretching vibration of the carbonyl group -C=O of enamelin collagenous proteins [3]. The broad band in the region $1700\text{--}1600\text{ cm}^{-1}$ is Amide I band, constituted from the bands at 1687 cm^{-1} , 1652 cm^{-1} and 1623 cm^{-1} . The amide I band at 1652 cm^{-1} is indicative of α -helical structure, although part of the absorption at this frequency also corresponds to random coil structure at 1623 cm^{-1} and antiparallel β -sheet at 1687 cm^{-1} [3, 15]. The decreased intensity of the characteristic band of α -helix structures in combination with the increased of those of β -sheet and carboxyl group band suggested that the high concentration of calcium leads to conformational changes of enamelin.

The band at 1584 cm^{-1} is assigned to asymmetric stretching vibration of carboxyl groups (νCOO^-) of proteins. The characteristic absorption band of Amide II due to the stretching vibrations C-N and bending vibration $\delta\text{N-H}$ was detected at about 1553 cm^{-1} . The band at 1520 cm^{-1} is related to the vibration of the tyrosine side chains [22].

Due to the high absorption of amide bands, DS enamel is accompanied by a high content of organic matrix and decrease in mineralization which leads to deficient enamel formation (hypomineralization) [22]. On the contrary the deconvolution analysis of healthy enamel revealed three bands at lower frequencies 1637 cm^{-1} , 1591 cm^{-1} and 1547 cm^{-1} , which are assigned to the vibrations of Amide I, carboxyl groups (νCOO^-) and Amide II of proteins, respectively. These spectral results are in agreement with the fact that enamel is characterized by a low abundance of proteins [1-4].

The band at 1463 cm^{-1} corresponds to the bending vibration of δCH_2 group which are overlapped from the absorption bands of carbonate group $\nu_3\text{CO}_3^{2-}$ of hydroxyapatite. The band at 1408 cm^{-1} in DS enamel and 1414 cm^{-1} for control enamel correspond to the stretching vibration of COO^- and $\nu_3\text{CO}_3^{2-}$ ions. DS enamel showed an intense band at 1243 cm^{-1} , which matched the spectra pattern of Amide III (in plane N-H bending and C-N stretching vibrations) [23]. No relative band was observed for healthy enamel.

The phosphate ion, PO_4^{3-} , is the principal molecular species giving rise to the HA absorbance in the region $900\text{--}1200\text{ cm}^{-1}$ (Fig. 3).

The bands at 1030 cm^{-1} in control enamel and 1014 cm^{-1} in DS enamel are assigned to the antisymmetric stretching mode of phosphate ions $\nu_{3as}\text{PO}_4^{3-}$ of hydroxyapatite group PO [16, 20, 24]. The band shift to lower wavenumbers is an indicator of the smaller crystals in Down syndrome patients. Furthermore, the shoulder band which is shown in the spectra of healthy enamel at 1085 cm^{-1} is attributed to antisymmetric stretching vibration of hydroxyapatite $\nu_3\text{PO}_4^{3-}$ group. This band in DS enamel spectra showed a red shift at 1099 cm^{-1} concerning less mature enamel, due to the molecular structure and development of mineral environment, the crystallinity and crystal size [25]. The shoulder bands at 966 cm^{-1} and 960 cm^{-1} for DS enamel and control enamel, respectively, are assigned to the antisymmetric stretching $\nu_1\text{PO}_4^{3-}$ vibration [3, 16, 21].

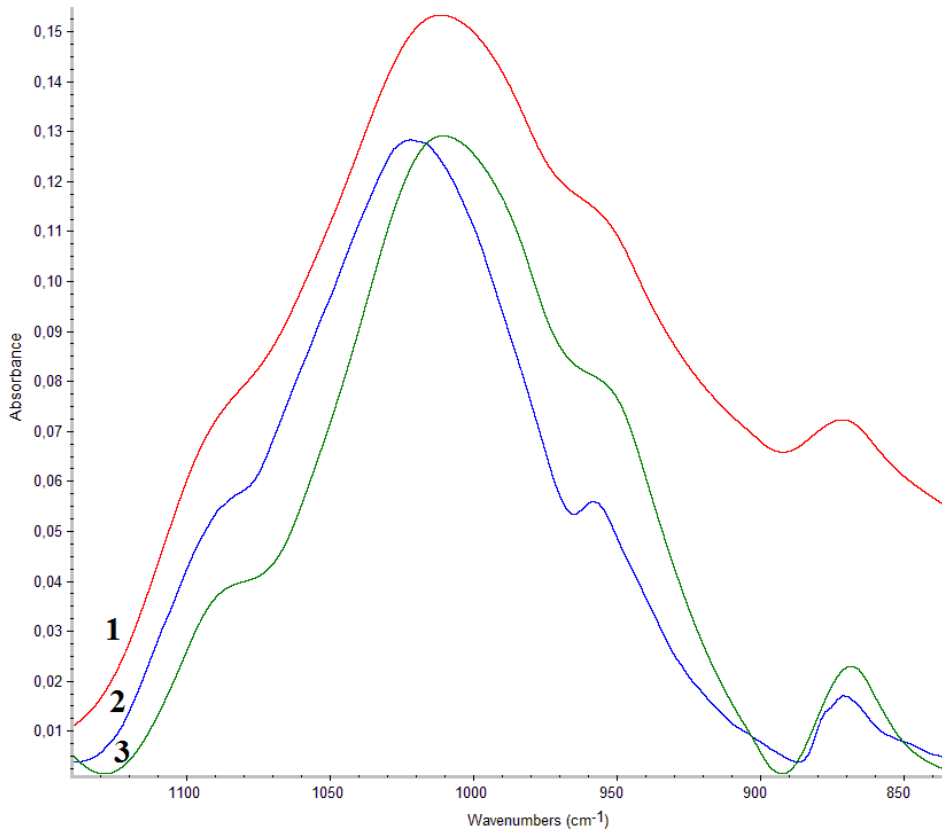


Figure 3. FT-IR absorption spectra of enamel obtained from; (1) DS (2) adult and (3) control children in the region 1200-800 cm^{-1} .

The absorption band at about 874 cm^{-1} present at three samples is attributed to the stretching vibration of carbonate ions $\nu_2\text{CO}_3^{2-}$. These data lead to the result that calcium carbonates exists in type B and have replaced phosphate ions νPO_4^{3-} in hydroxyapatite [17]. The following bands, at 604 and 567 cm^{-1} in enamel are due to the bending vibration of phosphate ions $\nu_4\text{PO}_4^{3-}(\text{O}-\text{P}-\text{O})$ [13, 17]. The spectra data confirmed that enamel consists mainly from inorganic compounds due to the low intensity of the amide bands of proteins in the region $1650\text{-}1240 \text{ cm}^{-1}$.

To the contrary, DS enamel contains organic compounds, as it is shown from the presence of the amide bands of collagen proteins. In the primary teeth, the presence of carbonate ions of calcium is more intense in comparison with the older teeth as it was demonstrated by the bands at 1455 cm^{-1} and 874 cm^{-1} . Finally, DS hydroxyapatite crystals are smaller in size in comparison those of health enamel and the crystallization has changed from biological to amorphous or mineral hydroxyapatite [13, 24, 25].

3.2. SEM analysis

SEM-EDX has been widely used to evaluate the morphology and elemental content of dental enamel. Significant differences were revealed between SEM images in the control enamel and DS enamel. Surface SEM images of enamel are shown in figure 5. The normal enamel indicated an ordered appearance with hydroxyapatite crystals forming rods and interrod enamel (Fig 4A &B) [28].

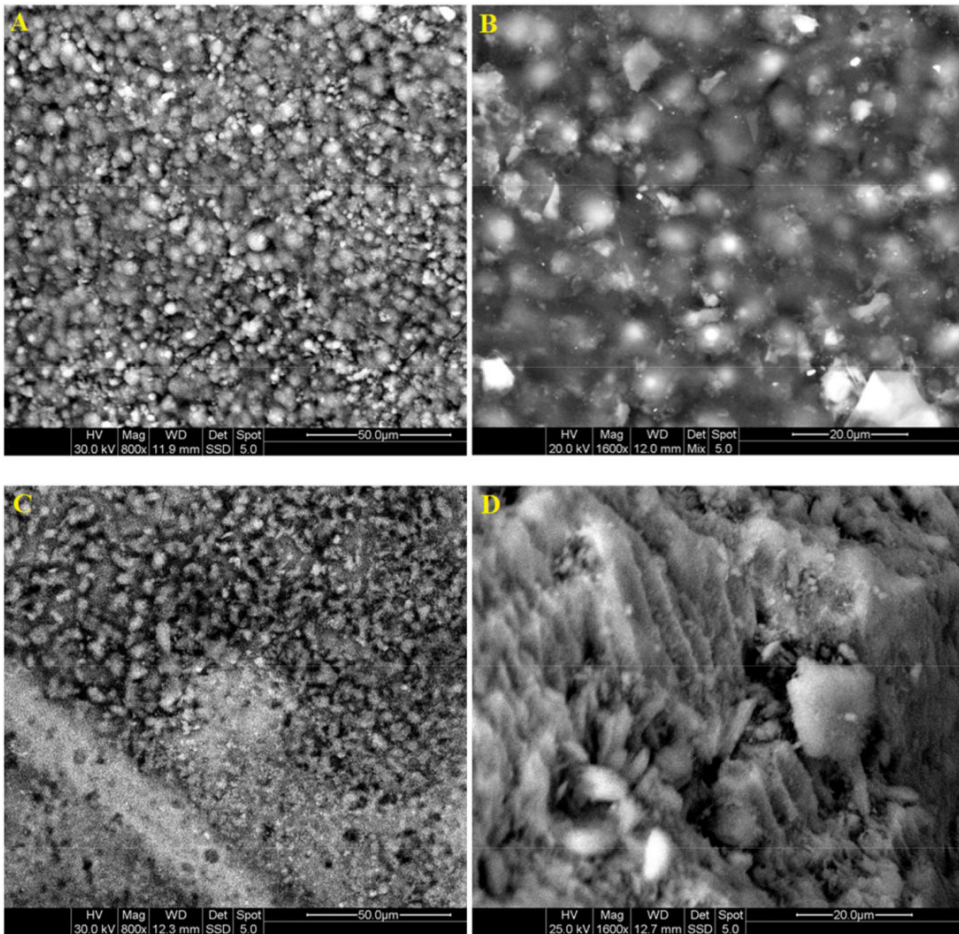


Figure 4. SEM imaging of surface enamel. A) Outer enamel layer in control children (800x magnification) B) Normal enamel typically displayed and well-organized crystallites (1600x magnification) C) Outer enamel layer in DS children (800x magnification) D) DS Enamel demonstrated area of amorphous material (1600x magnification).

In contrast, DS enamel was disorganized, the crystals were irregularly orientated and difficult to distinguish (Fig. 4C). At higher magnification, DS enamel has irregularly shaped porous

and prismatic structure. There were also observed white mineralized zones in enamel surface due the transformation of hydroxyapatite from biological to mineral structure.

This was also confirmed from the FT-IR spectra due to the increase of Amide III and δCH_2 bands. Amorphous material that did not demonstrate any crystallite was observed in the DS teeth but not in any of the control teeth examined (Fig.4D).

EDX analysis was used to determine the elemental components in enamel tissues. Apart from Ca and P which are the main components of hydroxyapatite, Na, Mg and Cl were also indicated in the analysis. Carbon and oxygen comes from the organic matrix and carbonate ions. The ratio of Ca/ P ranged from 1.91 to 2.04 in normal enamel and 1.77 to 1.96 in DS enamel. The lower concentration of Ca is due to the greater content of organic material in DS enamel [28]. The presence of Mg has been shown to be selectively acquired in the transitional stage. The selective uptake of magnesium reaches a maximum at the beginning of maturation due to association with enamel proteins. Crystal development includes a reduction in magnesium, carbonate and fluoride [22, 28]. DS enamel indicated high concentration of magnesium, which is related to high protein concentrations, resulting from insufficient mineralization. EDX analysis showed that the content of Mg varied from 0.4 to 0.55% in control enamel and 1.18 to 1.47% for DS enamel. Finally, DS enamel was altered both quantitatively and qualitatively, suggesting that protein dysfunction may result in enamel abnormalities in its structure and composition.

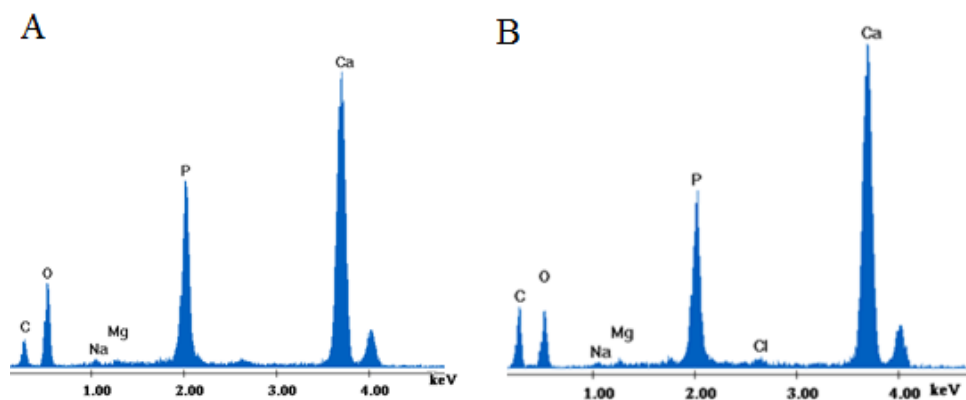


Figure 5. EDX analysis of healthy (A) and DS (B) enamel in an area surface

SEM observations were made on supragingival calculus, which is a product of calcification of dental plaque. In DS teeth, attached calculus formed a homogenous surface with calcified deposits. The calculus crystals were packed together with minimum porosity (Fig.6). In control teeth, supragingival calculus revealed a higher level of porosity with empty spaces due to the presence of microorganisms during the calcification process (Fig.6). Rod-like microorganisms could be identified in the calcified surfaces [29].

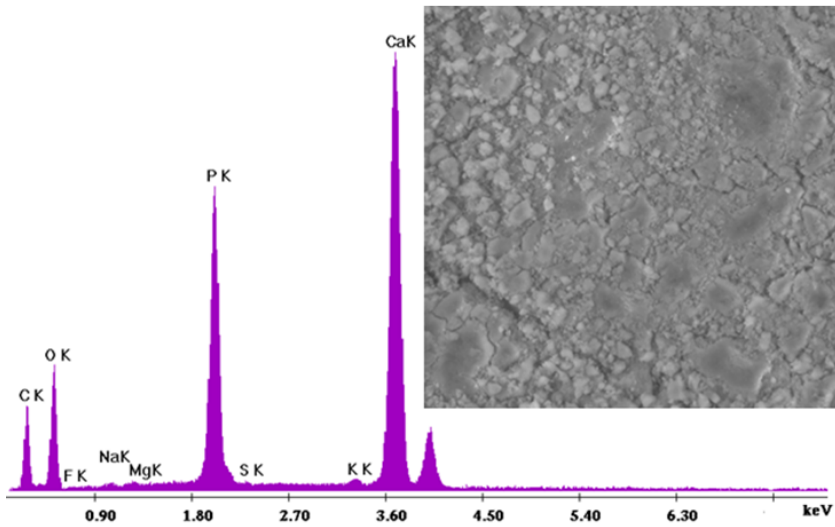


Figure 6. SEM imaging of DS enamel, region rich in mineral deposits (scale 300 μm) and their EDAX analysis of the area.

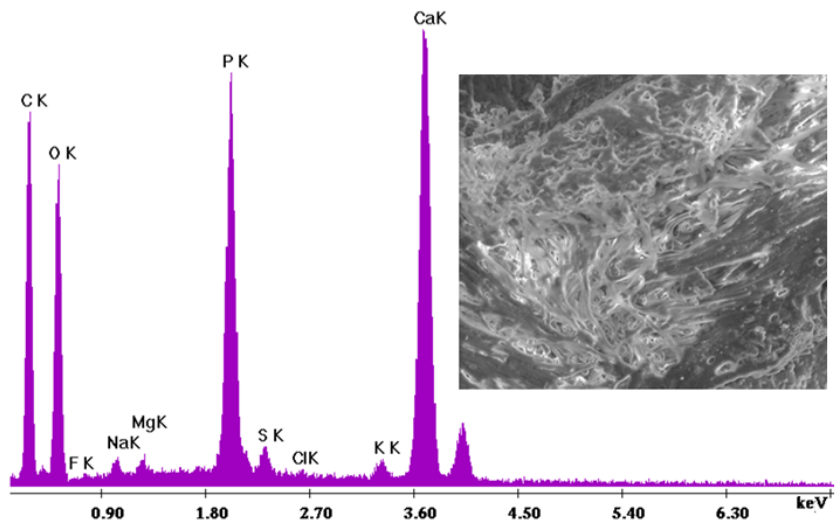


Figure 7. SEM imaging of control enamel, region rich in rod-like microorganisms (scale 300 μm) and their EDAX analysis of the area.

The presence of microorganisms in control teeth was also confirmed by EDX analysis. Apart from the main constituents of plaque such as Ca, P, C, O, high concentration of sulphur in

healthy patients was detected in contrast with Down syndrome patients. The presence of sulfur is characteristic feature of bacteria, which contain in their amino acids sulfur groups, leading to a diverse community of microorganisms found on the tooth surface of healthy patients [7, 30, 31].

It is suggested that the alterations in the structure of enamel of patients with Down syndrome may influence the attachment of oral bacteria in order to colonize and form biofilm due to high calcium concentration [32].

4. Conclusions

The investigation of enamel structure in children with Down Syndrome (DS) was carried out using Fourier Transform Infrared Spectroscopy (FT-IR) and Scanning Electron Microscopy (SEM) in combination with EDX. FT-IR spectroscopy allowed the analysis at the molecular level leading to the correlation of mineral content and organic matrix with enamel structure. High concentration of organic compounds was indicated in enamel from DS children teeth due to the lower degree of calcification. On the contrary, the low absorbance of amide bands in healthy children's enamel confirmed the lower composition of organic compounds. DS hydroxyapatite crystals were smaller in size to the health enamel crystals, while the molecular structure changed from biological to amorphous or mineral one, as it was demonstrated by SEM analysis. Supragingival calculus showed significant differences in morphology between the healthy and Down syndrome patients, as well as differences in elemental composition. In healthy patients, high concentration of sulphur was detected in contrast with Down syndrome patients. On the tooth surface of healthy patients, the presence of bacteria was detected. Further evaluation of dental samples from different groups of patients is required in order to identify the structural and composition variations of enamel and the mechanism of these abnormal features.

Author details

V. Dritsa^{1*}, D. Sgouros¹, K. Pissaridi², P. Bochlogyros¹, M. Kyriakidou¹ and V. Mamareli³

*Address all correspondence to: vdritsa@central.ntua.gr

1 National Technical University of Athens, Chemical Engineering Department, Radiation Chemistry & Biospectroscopy, Zografou Campus, Athens, Greece

2 University of Patras, Department of Chemistry, Food Chemistry and Technology, Greece

3 University of Patras, School of Medicine, Greece

References

- [1] Moradian-Oldak J. Amelogenins: assembly, processing and control of crystal morphology. *Matrix Biology* 2001; 20: 293-305.
- [2] Margolis HC, Beniash E, Fowler CE. Role of macromolecular assembly of enamel matrix proteins in enamel formation. *Journal of Dental Research* 2006; 85: 775-793.
- [3] Fan D, Lakshminarayanan R, Moradian-Oldak J. The 32 kDa enamelin undergoes conformational transitions upon calcium binding. *Journal of Molecular Structure* 2008; 163: 109-115.
- [4] Marshall GW, Marhsall SJ, Kinney JH, Balooch M. The dentin substrate: structure and properties related to bonding. *Journal of Dentistry* 1997; 25: 441-458.
- [5] Scheie A. *Advances in Dental Research* 1994; 8: 246-253.
- [6] Nyvad B, Fejerskov O. Structure of Dental Plaque and the Plaque-Enamel Interface in Human Experimental Caries. *Caries Research* 1989; 23: 151-158.
- [7] Marsh P D. Dental plaque: biological significance of a biofilm and community lifestyle. *Journal of Clinical Periodontology* 2005; 3: 7-15.
- [8] Rose RK, Turner SJ, Dibidin GH. Effect of pH and calcium concentration on calcium diffusion in streptococcal model-plaque biofilms. *Archives of Oral Biology* 1997; 42:795-800.
- [9] Shapiro BL. Prenatal dental anomalies in mongolism: comments on the basis and implications of variability. *Annals of the New York Academy of Science* 2006; 171: 562-577.
- [10] Zilberman U, Patricia S, Kupietzky A, Mass E. The effect of hereditary disorders on tooth components: a radiographic morphometric study of two syndromes. *Archives of Oral Biology* 2004;49: 621-629
- [11] Desai SS. Down syndrome: A review of the literature. *Oral Surgery, Oral Medicine, Oral Pathology Oral Radiology and Endodontology* 1997;84: 279-285
- [12] Theophanides T. *Infrared and Raman Spectra of Biological Molecules*. NATO Advanced Study Institute, D. Reidel Publishing Co, Dodrecht;1978.
- [13] Kolovou P, Anastassopoulou J. *Brilliant Light in Life and Material Sciences*. In: Tsakanov V, Wiedemann H (ed.) New York: Springer; 2007. p 267-272.
- [14] Anastassopoulou J, Boukaki E, Conti C, Ferraris P, Giorgini E, Rubini C, Sabbatini S, Theophanides T, Tosi G. Microimaging FT-IR spectroscopy on pathological breast tissues. *Vibrational Spectroscopy* 2009; 51: 270-275.
- [15] Conti C, Ferraris P, Giorgini E, Rubini C, Sabbatini S, Tosi G, Anastassopoulou J, Arapantoni P, Boukaki E, Theophanides T, Valavanis C. FT-IR Microimaging Spec-

- troscopy:Discrimination between healthy and neoplastic human colon tissues. *Journal of Molecular Structure* 2008; 881: 46-51.
- [16] Dritsa V. FT-IR spectroscopy in medicine. In Theophanides T. (ed.). *Infrared Spectroscopy-Life and Biomedical Sciences*. Croatia: Intech; 2012. p271-288.
- [17] Petra M, Anastassopoulou J, Theologis T, Theophanides T. Synchrotron micro-FT-IR spectroscopic evaluation of normal paediatric human bone, *Journal of Molecular Structure* 2005;. 78: 101-110.
- [18] Nyquist RA, Kagel RO. *Infrared spectra of inorganic compounds*. New York: Academic Press; 1971.
- [19] Bellamy LJ. *The Infrared Spectra of Complex Molecules*. New York: Wiley; 1958.
- [20] Theophanides T. *Fourier transform infrared spectroscopy*. Dordrecht: D. Reidel Publishing Co; 1984.
- [21] Petra M, J. Anastassopoulou J, Dovas A, Yfantis D, T. Aging of human bones. An infrared study. In: Centano JA. (ed), *Metal Ions in Biology and Medicine*, 2000. p736-
- [22] Mamarelis I, Pissaridi K, Dritsa V, Kotileas P, Tsigiliris V, Anastassopoulou J. Oxidative Stress and Atherogenesis. An FT-IR Spectroscopic Study. *In Vivo* 2010; 24: 883-888.
- [23] Theophanides T, Angiboust JP, Manfait M. In: Twardowski H.(ed.) *Spectroscopic and Structural Studies of Biomaterials I: Proteins.*, Wilmslow: Sigma Press; 1988.
- [24] Gadaleta SJ, Paschalis EP, Betts F, Mendelsohn R, Boskey AL. New Infrared Spectra Structure Correlations in the Amorphous Calcium Phosphate to Hydroxyapatite Conversion. *Calcified Tissue International* 1996; 38: 9-16.
- [25] Bohic S, Heymann D, Pouezat JA, Gauthier O, Dalcusi G. Transmission FT-IR micro-spectroscopy of mineral phases in calcified tissues. *C R Acad. Paris* 1998; 321: 865-876.
- [26] Robinson C, Kirkham J, Brookes J, Bonass WA, Shore RC. Chemistry of Enamel Development. *International Journal of Developmental Biology*, 1995; 39: 145-152.
- [27] Mahoney EK, Rohanizadeh R, Ismail FSM, Kilpatrick NM, Swain MV. Mechanical properties and microstructure of hypomineralised enamel of permanent teeth. *Biomaterials* 25, 5091 (2004).
- [28] Wright JT, Robinson C, Shore R. Characterization of the enamel ultrastructure and mineral content in hypoplastic amelogenesis imperfecta. *Oral Surgery, Oral Medicine and Oral Pathology* 1991; 72: 594-601.
- [29] Lustmann J, Lewin-Epstein J, Shteyer A. Scanning electron microscopy of dental calculus. *Calcified Tissue Research* 1976; 21(1): 47-55.

- [30] Zee KY, Samaranayke LP, Attstrom R. Scanning electron microscopy of microbial colonization of 'rapid' and 'slow' dental-plaque formers in vivo. *Archives of Oral Biology* 1997;42: 735-742.
- [31] He B, Huang S, Zhang C, Jing J, Hao Y, Xiao L, Zhou X. Mineral densities and elemental content in different layers of healthy human enamel with varying teeth age. *Archives of Oral Biology* 2011; 56: 997-1004.
- [32] Theodorakopoulou O, Anastassopoulou J. Influence of traditional mathematics and mechanics on modern science and technology. In : Sih GC, Spyropoulos CP (ed), *Ep-talofos, SA*, 2004. p.453-462.

